Termination of global warmth at the Palaeocene/Eocene boundary through productivity feedback

Santo Bains*, Richard D. Norris†, Richard M. Corfield* & Kristina L. Faul‡

** Department of Earth Sciences, Parks Road, University of Oxford, Oxford OX1 3PR, UK*
† Department of Geology and Geophysics, Woods Hole Oceanographic Institution, Woods Hole, Massachusetts 02540-1541, USA
‡ Earth Sciences Department, University of California, Santa Cruz, California 95064, USA

The onset of the Palaeocene/Eocene thermal maximum (about 55 Myr ago) was marked by global surface temperatures warming by 5–7 °C over approximately 30,000 yr (ref. 1), probably because of enhanced mantle outgassing[2,3] and the pulsed release of ~1,500 gigatonnes of methane carbon from decomposing gas-hydrate reservoirs[4–7]. The aftermath of this rapid, intense and global warming event may be the best example in the geological record of the response of the Earth to high atmospheric carbon dioxide concentrations and high temperatures. This response has been suggested to include an intensified flux of organic carbon from the ocean surface to the deep ocean and its subsequent burial through biogeochemical feedback mechanisms[8]. Here we present firm evidence for this view from two ocean drilling cores, which record the largest accumulation rates of biogenic barium—indicative of export palaeoproductivity—at times of maximum global temperatures and peak excursion values of $\delta^{13}C$. The unusually rapid return of $\delta^{13}C$ to values similar to those before the methane release[7] and the apparent coupling of the accumulation rates of biogenic barium to temperature, suggests that the enhanced deposition of organic matter to the deep sea may have efficiently cooled this greenhouse climate by the rapid removal of excess carbon dioxide from the atmosphere.

Mean surface air temperatures at the end of the Palaeocene epoch were ~6.7–8.5 °C warmer than today[9]. Despite the already warm temperatures, this period in the Earth's history was punctuated by a ~60,000-year episode of intense global warming at the Palaeocene/Eocene (P/E) boundary[1,4,10]. It is likely that this warmth was caused primarily by increased atmospheric CO_2 concentrations released by tectonic events[2,3] and was related to the destabilization (and oxidation) of sea-floor gas-hydrate accumulations[4–7]. Gas hydrates are naturally occurring solids composed of mainly water and methane molecules, and are found in geographically diverse continental margin settings[11]. Low temperatures (< 7 °C) and high pressures (> 50 bar) maintain the crystalline lattices[11] of these hydrates, which are present in vast quantities today (of the order of 10^4 gigatonnes (Gt) of methane carbon, or double the estimate of carbon from all known fossil-fuel sources)[11]. Methane from gas hydrates has an average $\delta^{13}C$ of –60‰ (ref. 11), and its pulsed release at the P/E boundary is shown by a very marked, stepped, negative shift in the global $\delta^{13}C$ record that accompanied the rapid warming[4–7]. On a millennial timescale, the rate of greenhouse-gas emission at the P/E boundary is approximately comparable to current industrial levels, and thus provides a unique insight into our uncertain greenhouse future. In response to the changing conditions of the P/E boundary, marine and terrestrial organisms underwent a period of intense reorganization[12,13] including a notable extinction of about 50% of the species of benthic foraminifera in the deep sea[14].

The oceans contain about 60 times more carbon than the atmosphere, and it has been suggested that the CO_2 concentration of the atmosphere can be controlled by changes in the export productivity of the oceans[15]. During photosynthesis, marine phytoplankton fix CO_2 into their tissues; these tissues eventually settle to the deep sea (where they become part of the sedimentary organic matter) or are oxidized in transit[16]. The ocean surface water, depleted in CO_2, then re-equilibrates with the atmosphere[15,16]. The availability of nutrients (particularly P, N and Fe) in surface waters is often the limiting factor for primary productivity[17,18]. An increased input of nutrients—by, for example, upwelling from the deep sea—can cause blooms of phytoplankton, and increased export of carbon into the ocean interior: this is the process known as the 'carbon pump'. Here we present evidence of enhanced organic-matter production and burial in the oceans (via proposed biogeochemical feedback mechanisms[8]) following gas-hydrate dissociation at the P/E boundary, and suggest that this may have led to rapidly reduced global temperatures. A combination of optimal conditions (increased runoff from the continents[19], oceanic fertilization from volcanic fallout[2], rising global temperatures[1,4,20] and increased atmospheric CO_2 concentrations[2–7]) during the P/E thermal maximum seems to have triggered a bloom in marine phytoplankton, which may have sequestered the greenhouse gas CO_2 to the deep sea by about 60,000 years of enhanced biological 'pumping'[8].

Biogenic barium ($Ba_{biogenic}$) is well suited for use as a palaeoproductivity proxy. In the modern open ocean, the flux of $Ba_{biogenic}$ correlates well with export production (that is, organic-carbon flux from surface waters) in both sediment traps[21] and in deep-sea sediments[22]. In sediments, barite—the main carrier of Ba related to biological productivity[21]—is well preserved in pelagic settings and has a burial efficiency of 30% (refs 21, 23); it is not affected by diagenesis in oxic environments[24]. The refractory nature of barite is particularly useful for studying the P/E thermal maximum because

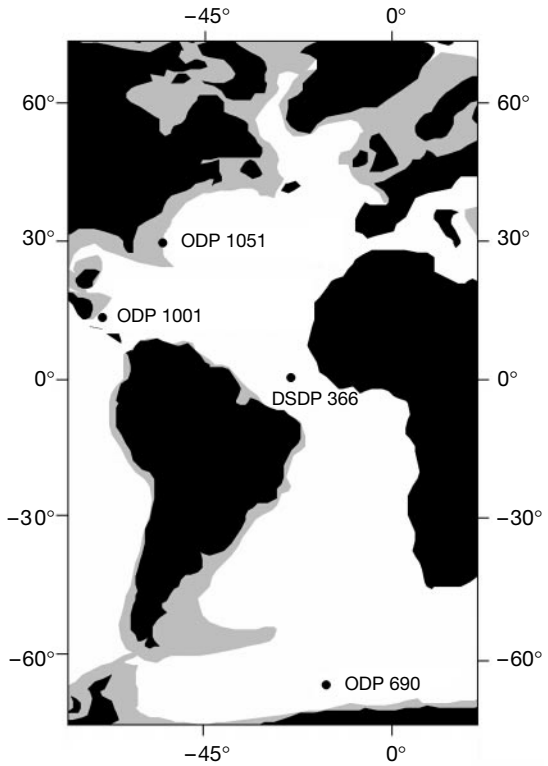

Figure 1 Palaeocene location of the sites analysed for biogenic-barium concentrations across the P/E boundary. DSDP 366: Sierra Leone rise, mid-Atlantic Ocean (present location: 05° 41′N, 19° 51′ W). ODP 690: Maud rise, Weddell Sea, Antarctica (present location: 65°09′ S, 01° 12′E). ODP 1001: lower Nicaraguan rise, Caribbean Sea (present location: 15° 45′ N, 74° 55′ W). ODP 1051: Blake nose, western North Atlantic Ocean (present location: 30° 03′ N, 76° 21′ W). Shaded areas indicate ocean depths less than 500 m below sea level.

other proxies (for example, $CaCO_3$, biogenic silica and organic carbon) are subject to significant remineralization and cannot comprehensively define the nature of productivity changes over this interval. Barite is thought to form in the upper water column[25], in microenvironments associated with decomposing organic matter such as the remains of siliceous plankton[26,27] and acantharian shells[27], or possibly from direct precipitation by living biological organisms[28]. Although the exact mechanism of barite formation remains a topic of debate, there is abundant evidence for a strong relationship between barite and export productivity in the modern ocean. Accordingly, in the palaeorecord, high accumulation rates of $Ba_{biogenic}$ in deep-sea drill cores are thought to correspond to episodes of increased export palaeoproductivity, and have thus been used as export productivity tracers throughout the Cenozoic[22,29]. For the purposes of our study, we calculate the flux of $Ba_{biogenic}$ and account for Ba from detrital sources by normalizing to Al (according to the method of Dymond *et al.*[21]).

We have determined the $Ba_{biogenic}$ concentrations of 130 marine samples across the P/E boundary, from two geographically diverse Ocean Drilling Program (ODP) sites 690 and 1051 (Fig. 1), and have converted these values into mass accumulation rates (MARs) using a well constrained high-resolution orbital timescale based on precessional cycles[10]. Our results clearly show that the decline of the global greenhouse climate coincided with an accelerated $Ba_{biogenic}$ flux at both ODP sites (Fig. 2). The calculated accumulation rates return to pre-excursion levels in a manner virtually identical to that of published $\delta^{18}O$ and $\delta^{13}C$ records[1,4].

Although $Ba_{biogenic}$ cannot be used to record accurately changes in export productivity under highly reducing conditions (because Ba remobilization may occur due to sulphate reduction), barite is well preserved in oxic sediments such as those studied here[24]. Additionally, Ba remobilization results in a negative inflection in $Ba_{biogenic}$, whereas the excursion that we observe is positive. Furthermore, the similarity of the $Ba_{biogenic}$ records and published $\delta^{13}C$ and $\delta^{18}O$

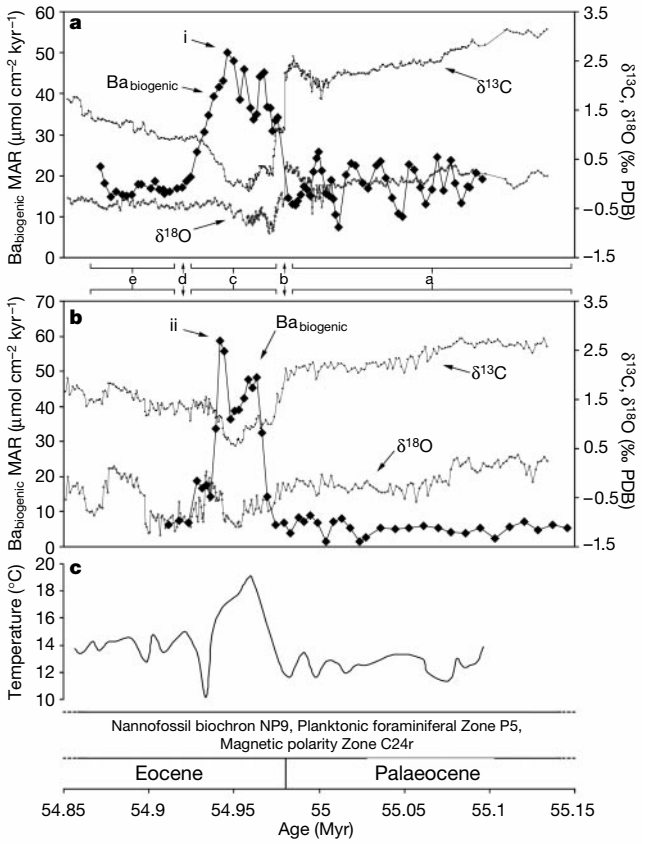

Figure 2 Variation across the P/E boundary of the properties of two deep-sea sediment cores. The figure shows biogenic-barium mass accumulation rate ($Ba_{biogenic}$ MAR), and $\delta^{13}C$ and $\delta^{18}O$ records[4] from ODP sites 690B (**a**,**c**) and 1051B (**b**). The Antarctic Ocean water temperature change (°C) throughout this interval closely resembles inferred export productivity variations at both sites (**c**). The temperature stratigraphy was generated from published benthic foraminifer *Nuttallides truempyi* $\delta^{18}O$ data[1]. Before the P/E boundary, the $Ba_{biogenic}$ flux remains relatively stable at sites 690B and 1051B (feature a). Following the initial burst of warmth and carbon-isotope excursion, $Ba_{biogenic}$ MARs dramatically increase in both the mid- and high-latitude Atlantic Ocean (feature b). $Ba_{biogenic}$ MARs rise from 6 to 48 μmol Ba cm^{-2} kyr^{-1} in ODP 1051B, and from 14 to 34 μmol Ba cm^{-2} kyr^{-1} in ODP 690B within ~ 5,000–7,000 years. Subsequently, for an interval of about 60,000 years (corresponding to the warmest interval of the P/E transition; feature c), $Ba_{biogenic}$ MARs remain high with peak flux of 59 μmol Ba cm^{-2} kyr^{-1} reached in the western North Atlantic Site 1051B (ii) and 50 μmol Ba cm^{-2} kyr^{-1} in the Antarctic Site 690B (i). Global temperatures trends vary with $Ba_{biogenic}$ MARs as the records return to near pre-excursion levels (feature d). The fact that $Ba_{biogenic}$ MARs stabilize at the same time in two geographically diverse cores strongly suggests that the mechanism that was driving enhanced export productivity became exhausted at all latitudes simultaneously. In the aftermath of this intense global warming (and cooling) anomaly, $Ba_{biogenic}$ MARs and global temperatures remain relatively stable into the early Eocene epoch (feature e). The fact that maximum $Ba_{biogenic}$ MARs are reached first in site 690B (i) could reflect the high-latitude oceans being more rapidly affected by changing atmospheric greenhouse-gas concentrations. Recent concerns that some Al in oceanic sediments might also be of biogenic origin[32] prompted us to verify the fidelity of our results by normalization using Ti. $Ba_{biogenic}$ concentrations obtained by this approach were virtually identical to those obtained using Al, and Al:Ti ratios indicated no Al from biogenic sources. All elemental abundance data were generated by inductively coupled plasma atomic emission spectrometry (ICP-AES) analysis of crushed bulk sediments dissolved in a 1:2 mixture of $HClO_4$ and HF acids, then diluted with HCl and distilled water.

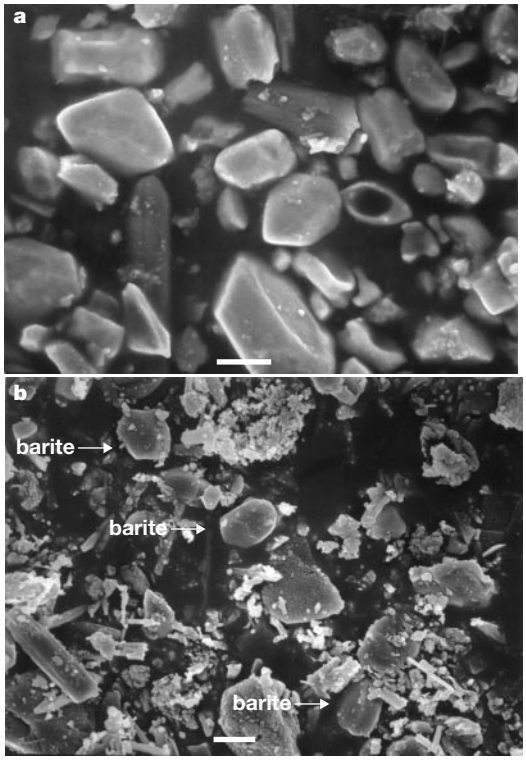

Figure 3 Scanning electron micrographs of marine barite microcrystals (1–5 μm in size) from samples during (**b**) and after (**a**) the P/E boundary. **a**, Sediment significantly above the P/E boundary from Site 1051A (171B 1051 A, 48X-4, 71–73 cm, depth 453 m below sea floor, m.b.s.f.); **b**, sediment from Site 1051B where $Ba_{biogenic}$ MAR values rapidly increase following the primary $\delta^{13}C$ excursion at the P/E boundary, 512.75 m.b.s.f., approximately 54.966 Myr ago. Sample **b** was used in this study, and in addition to the barite crystals, dissolution-resistant terrigenous particles are present, including titanium oxides and aluminosilicates. Each scale bar is ~ 2 μm.

data[1,4] suggest that all are largely controlled by perturbations in the carbon cycle and global climate at the P/E boundary. We believe, therefore, that the $Ba_{biogenic}$ MAR anomaly is not a diagenetic phenomenon. Diagenesis would be expected to strip Ba out of pore waters, and cause the baseline values following the excursion to be lower than before the excursion[30]. Our data from both sites rise from, and fall to, the same baseline values. Furthermore, we would expect $Ba_{biogenic}$ MARs to begin to increase below the onset of the $\delta^{13}C$ anomaly if the $Ba_{biogenic}$ MAR peak were due entirely to the diffusion of sulphate from underlying oxic sediments. To confirm that our samples contain biogenic barite, we separated marine biogenic barite in selected samples using the method of Paytan *et al.*[24], and observed distinct ovoid barite crystals using scanning electron microscopy and elemental analysis (SEM/EDS) in samples from site 1051B taken from the P/E thermal maximum interval, and from site 1051A slightly above the interval (Fig. 3). Barite crystals with this type of morphology have been identified in sediments underlying other ancient high-productivity regions[24]. The exceptional preservation of these crystals in both samples strongly suggests that our $Ba_{biogenic}$ MAR findings reflect ancient surface export production, and that neither Ba remobilization nor diagenesis has significantly affected our records.

Recent analysis using mass-balance equations suggests that the recovery of the $\delta^{13}C$ record at ODP site 1051 occurred more rapidly than would be expected through a steady-state carbon cycle[7]. The most plausible explanation for this would be a global increase in carbon throughput and organic-carbon burial following gas-hydrate dissociation[7]. The similarity in shape of the $\delta^{13}C$ and $Ba_{biogenic}$ records at both sites (an abrupt excursion followed by a gradual return to base levels) indicates that $Ba_{biogenic}$ can indeed be used as an export productivity proxy, and that our findings are consistent with the operation of a globally enhanced biological 'pump' that preferentially sequestered large quantities of ^{12}C to the ocean depths, stimulated by changes to the global climate and carbon cycle during the P/E thermal maximum.

Both ODP sites used in our study are near continental landmasses, suggesting that our data could reflect an export productivity and burial phenomenon at depositional environments of this sort world-wide, as the Earth's carbon cycle laboured to reach equilibrium following massive input of CO_2 to the atmosphere. A strong productivity signal in eastern Tethys during the late Palaeocene, thought to be due primarily to vigorous upwelling[29], may also have been caused by the mechanism we report here. In further support of the global scale of the biological response that we discuss, preliminary work has shown elevated Ba concentrations in Caribbean (ODP 1001) and eastern tropical Atlantic (DSDP 366) sediments that contain the P/E boundary.

Some previous studies of P/E boundary sections have suggested decreased productivity[13,20]. Nonetheless, in the modern ocean, regional oceanographic conditions can vary significantly, and it is not unlikely that there was an overall increase in carbon burial even if some sites became oligotrophic. The structure of complete $\delta^{13}C$ records from the P/E boundary (ref. 4), and their faster-than-expected recovery to pre-excursion levels[7] (coupled with our $Ba_{biogenic}$ records), transcend regional variations, and indicate an increase in the global-average organic matter export and burial.

It is probable that much of the organic matter deposition associated with the P/E boundary occurred in near-shore marine environments[8]. As the climate became very humid and wet, increased rainfall could have caused enhanced erosion of the continents (from chemical weathering), and may have led to a boost in the nutrient supply to the oceans from terrestrial runoff[8]. This, coupled with increased temperatures and atmospheric CO_2 concentrations, and fertilization by volcanic fallout, could have caused blooms in many oceanic regions. We also note that, although the ocean is the largest sink for atmospheric CO_2, P/E boundary conditions were probably also favourable for the increased abundance of terrestrial biota (particularly plants) and carbon-bearing soils, which almost certainly would have further accelerated the recovery of the global carbon cycle as geographic coverage increased[8,31].

We have shown the existence of an export productivity maximum at the P/E boundary, lending support to the theory that these conditions produced a series of negative feedbacks[8] in the climate system. These feedbacks acted as an immense 'biological pump', effectively reducing the increased atmospheric concentration of greenhouse gases and rapidly returning the Earth to average late Palaeocene conditions. It is possible that biological activity of this type might eventually reduce the atmospheric concentrations of CO_2 that are at present rising due to anthropogenic emissions. However, we note that it took ~60,000 years for late Palaeocene temperatures to return to normal following the apparently cataclysmic decomposition of gas hydrates. Furthermore, the current potential of the 'biological pump' may have been reduced by deforestation and pollution of the oceans. □

Received 6 March; accepted 17 July 2000.

1. Kennett, J. P. & Stott, L. D. Abrupt deep-sea warming, palaeoceanographic changes and benthic extinctions at the end of the Palaeocene. *Nature* **353,** 225–229 (1991).
2. Eldholm, O. & Thomas, E. Environmental impact of volcanic margin formation. *Earth Planet. Sci. Lett.* **117,** 319–329 (1993).
3. Rea, D. K., Zachos, J. C., Owen, R. M. & Gingerich, P. D. Global change at the Paleocene-Eocene boundary: climatic and evolutionary consequences of tectonic events. *Palaeogeogr. Palaeoclimatol. Palaeoecol.* **79,** 117–128 (1990).
4. Bains, S., Corfield, R. M. & Norris, R. D. Mechanisms of climate warming at the end of the Paleocene. *Science* **285,** 724–727 (1999).
5. Dickens, G. R., O'Neil, J. R., Rea, D. K. & Owen, R. M. Dissociation of oceanic methane hydrate as a cause of the carbon isotope excursion at the end of the Paleocene. *Paleoceanography* **10,** 965–971 (1995).
6. Dickens, G. R., Castillo, M. M. & Walker, J. C. G. A blast of gas in the latest Paleocene: Simulating first-order effects of massive dissociation of oceanic methane hydrate. *Geology* **25,** 259–262 (1997).
7. Dickens, G. R. Carbon addition and removal during the Late Palaeocene Thermal Maximum: Basic theory with a preliminary treatment of the isotope record at Ocean Drilling Program Site 1051, Blake Nose. In *Western North Atlantic Palaeogene and Cretaceous Paleoceanography* (eds Kroon, D., Norris, R. D. & Klaus, A.)(Special Publication, Geological Society, London, in the press).
8. Zachos, J. C. & Dickens, G. R. An assessment of the biogeochemical feedback response to the climatic and chemical perturbations of the LPTM. *GFF* **122,** 188–189 (2000).
9. Budyko, M. Climate catastrophes. *Glob. Planet. Change* **20,** 281–288 (1999).
10. Norris, R. D. & Röhl, U. Carbon cycling and chronology of climate warming during the Palaeocene/Eocene transition. *Nature* **401,** 775–778 (1999).
11. Kvenvolden, K. A. in *Gas Hydrates* (eds Henriet, J. -P. & Mienert, J.) 9–30 (Geological Society, London, 1998).
12. Koch, P. L., Zachos, J. C. & Gingerich, P. D. Correlation between isotope records in marine and continental carbon reservoirs near the Palaeocene/Eocene boundary. *Nature* **358,** 319–322 (1992).
13. Kelly, D. C., Bralower, T. J. & Zachos, J. C. Evolutionary consequences of the latest Paleocene thermal maximum for tropical planktonic foraminifera. *Palaeogeogr. Palaeoclimatol. Palaeoecol.* **141,** 139–161 (1998).
14. Pak, D. K. & Miller, K. G. Late Paleocene to early Eocene benthic foraminiferal stable isotopes and assemblages: implications for deepwater circulation. *Paleoceanography* **7,** 405–422 (1992).
15. Broecker, W. S. Glacial to interglacial changes in ocean chemistry. *Prog. Oceanogr.* **11,** 151–197 (1982).
16. Corfield, R. M. Palaeocene oceans and climate: An isotopic perspective. *Earth-Sci. Rev.* **37,** 225–252 (1994).
17. Tyrrell, T. The relative influences of nitrogen and phosphorus on oceanic primary production. *Nature* **400,** 525–531 (1999).
18. Falkowski, P. G., Barber, R. T. & Smetacek, V. Biogeochemical controls and feedbacks on ocean primary production. *Science* **281,** 200–206 (1998).
19. Robert, C. & Kennett, J. P. Antarctic subtropical humid episode at the Paleocene-Eocene boundary: clay-mineral evidence. *Geology* **22,** 211–214 (1994).
20. Thomas, D. J., Bralower, T. J. & Zachos, J. C. New evidence for subtropical warming during the late Paleocene thermal maximum: Stable isotopes from Deep Sea Drilling Project Site 527, Walvis Ridge. *Paleoceanography* **14,** 561–570 (1999).
21. Dymond, J., Suess, E. & Lyle, M. Barium in deep-sea sediment: A geochemical proxy for productivity. *Paleoceanography* **7,** 163–181 (1992).
22. Paytan, A., Kastner, M. & Chavez, F. P. Glacial to interglacial fluctuations in productivity in the Equatorial Pacific as indicated by marine barite. *Science* **274,** 1355–1357 (1996).
23. Paytan, A. & Kastner, M. Benthic Ba fluxes in the central Equatorial Pacific, implications for the oceanic Ba cycle. *Earth Planet. Sci. Lett.* **142,** 439–450 (1996).
24. Paytan, A., Kastner, M., Martin, E. E., Macdougall, J. D. & Herbert, T. Marine barite as a monitor of seawater strontium isotope composition. *Nature* **366,** 445–449 (1993).
25. Legeleux, F. & Reyss, J. $^{228}Ra/^{226}Ra$ activity ratio in oceanic settling particles: implications regarding the use of barium as a proxy for paleoproductivity reconstruction. *Deep-Sea Res. I* **43,** 1857–1863 (1996).
26. Bishop, J. K. B. The barite-opal-organic carbon association in oceanic particulate matter. *Nature* **332,** 341–343 (1988).
27. Bernstein, R. E., Byrne, R. H. & Schijf, J. Acantharians: a missing link in the oceanic biogeochemistry of barium. *Deep-Sea Res. I* **45,** 491–505 (1998).

28. Bertram, M. A. & Cowen, J. P. Morphological and compositional evidence for biotic precipitation of marine barite. *J. Mar. Res.* **55,** 577–593 (1997).
29. Schmitz, B., Charisi, S. D., Thompson, E. I. & Speijer, R. P. Barium, SiO_2 (excess), and P_2O_5 as proxies of biological productivity in the Middle East during the Palaeocene and the latest Palaeocene benthic extinction event. *Terra Nova* **9,** 95–99 (1997).
30. McManus, J. *et al.* Geochemistry of barium in marine sediments: Implications for its use as a paleoproxy. *Geochim. Cosmochim. Acta* **62,** 3453–3473 (1998).
31. Beerling, D. J. The responses of the terrestrial carbon cycle to global change across the Paleocene/Eocene boundary. *GFF* **122,** 23 (2000).
32. Murray, R. W., Leinen, M. & Isern, A. R. Biogenic flux of Al to sediment in the central Equatorial Pacific Ocean: Evidence for increased productivity during glacial periods. *Paleoceanography* **8,** 651–670 (1993).

Acknowledgements

We thank N. Paige, S. James, N. Walsh, S. Wyatt and J. Cartlidge for their technical assistance; and G. Dickens, M. Delaney and A. Paytan for discussions and comments. We also thank A. Paytan for use of her laboratory to separate barite. Samples for this study were taken from cores drilled and supplied by the Ocean Drilling Program. The Natural Environment Research Council (UK), NSF and JOI/USSP supported this work.

Correspondence and requests for data should be addressed to S.B. (e-mail: santo.bains@earth.ox.ac.uk).

Earthquake-induced changes in a hydrothermal system on the Juan de Fuca mid-ocean ridge

H. Paul Johnson*, Michael Hutnak*, Robert P. Dziak†, Christopher G. Fox†, Istvan Urcuyo‡, James P. Cowen§, John Nabelek‖ & Charles Fisher‡

* *School of Oceanography, University of Washington, Seattle, Washington 98195-7940, USA*
† *PMEL NOAA and Oregon State University, Newport, Oregon 97365, USA*
‡ *Department of Biology, Pennsylvania State University, University Park, Pennsylvania 16802, USA*
§ *Department of Oceanography, University of Hawaii, Honolulu, Hawaii 96822, USA*
‖ *COAS, Oregon State University, Corvallis, Oregon 97331, USA*

Hydrothermal vents on mid-ocean ridges of the northeast Pacific Ocean are known to respond to seismic disturbances, with observed changes in vent temperature[1–4]. But these disturbances resulted from submarine volcanic activity; until now, there have been no observations of the response of a vent system to non-magmatic, tectonic events. Here we report measurements of hydrothermal vent temperature from several vents on the Juan de Fuca ridge in June 1999, before, during and after an earthquake swarm of apparent tectonic origin. Vent fluid temperatures began to rise 4–11 days after the first earthquake. Following this initial increase, the vent temperatures oscillated for about a month before settling down to higher values. We also observed a tenfold increase in fluid output from the hydrothermal system over a period of at least 80 days, extending along the entire ridge segment. Such a large, segment-wide thermal response to relatively modest tectonic activity is surprising, and raises questions about the sources of excess heat and fluid, and the possible effect on vent biological communities.

The earthquake swarm occurred on 8 June, and was located on the Endeavour segment of the Juan de Fuca ridge (Fig. 1a), a well studied spreading centre with extensive hydrothermal activity (Fig. 1b; ref. 5), but one that lacks evidence of recent volcanic activity. Unlike the southern Juan de Fuca ridge, the Endeavour segment is very active seismically, producing hundreds of small (magnitude $M < 4$) earthquakes per year. Seismicity from submarine volcanic events is characterized by steady, low-level earthquakes, horizontal migration of epicentres due to lateral dyke injection, and continuous, low-frequency volcanic tremor. In contrast, earthquakes generated by non-magmatic, tectonic movements along normal or strike-slip faults are also frequent in the northeast Pacific, and are characterized by a large initial main shock, followed by aftershocks that decay quasi-exponentially through time with no associated volcanic tremor. The 8 June earthquake is interpreted to be tectonic in origin because the initial earthquake was the largest of the swarm, there was quasi-exponential decay in the number of aftershocks, and volcanic tremor was absent. This event was significantly more intense than similar tectonic sequences observed at the Endeavour segment, with a main shock of magnitude 4.5 and an unusually large number of aftershocks occurring during five days of activity (Fig. 1a). The main shock was recorded by the Pacific Northwest regional seismic network, and the focal mechanism was determined using moment tensor inversion techniques[6] to be the result of slip on a normal fault striking 160°, further supporting the tectonic origin of this event.

That the 8 June event was 'non-eruptive' is strongly suggested by data obtained during extensive dives by the submersibles *Alvin* and *Jason* during August–September 1999 in the Endeavour axial valley: no evidence was found of any new volcanic activity in multiple vehicle traverses between the Beach and Clam Bed sites (see Fig. 1 for locations). However, a great increase of particulate matter in the bottom water was observed at all sites during these dives, compared to previous years. A ubiquitous white flocculent material was suspended in the near-bottom water and covered much of the areas of diffuse flow; several diffuse vents were still emitting this material in August–September. Microscopic examination confirmed that the flocculent material was largely inorganic, presumably sulphur of biogenic origin (D.C. Nelson, personal communication), similar to that reported coming from 'snow-blower vents', which accompany crustal disturbances associated with submarine eruptions[7,8]. Most of the 8 June aftershock seismicity had ceased by 13 June.

The earthquake locations shown in Fig. 1a indicate that the locus of seismic activity is offset to the west of the Endeavour axial valley, with a mean event location (weighted by epicentral uncertainty) of 47° 52.4′ N and 129° 14.2′ W. A bias in epicentre locations is possible due to sound velocity or bathymetry effects, but the distribution of locations indicate that the swarm was probably centred 7.5 km west of the segment axis. This area of the Endeavour western flank has large, exposed, inward-facing fault scarps associated with crustal stretching that have been observed during previous *Alvin* dives[9].

During the 10-month interval preceding 8 June, hydrothermal vent temperatures on the Endeavour segment were monitored at the Easter Island site (EI/MEF, within the main Endeavour field) and the Clam Bed site (650 m south of the High Rise field). At these locations, water temperatures associated with *vestimentiferan* tubeworm aggregations around diffuse vents were monitored using four pairs of thermistors, with the lower (near-bottom) sensor of each pair embedded among the bases of the tubeworms within diffuse flow, and the upper sensor near the plumes of the tubeworms, approximately 0.5 m above the sea floor. The Beach site (300 m south of the MEF) is a small sediment pond within the axis, with diffuse hydrothermal fluid venting around and through the sediments. At this site, a bio-column installation was filtering hydrothermal fluids to isolate sub-surface microbial populations, and the hydrothermal effluent was contained entirely within the plumbing of the enclosed bio-filter system. The hydrothermal fluid temperatures were measured within a PVC filter shell, isolated from normal bottom-water variations. The bio-column data logger also had a companion external thermistor for measuring the general